

LS-DYNA Air Blast Techniques: Comparisons with Experiments for Close-in Charges

Len Schwer¹, Hailong Teng², Mhamed Souli³

¹Schwer Engineering & Consulting Services

²Livermore Software Technology Corporation

³University of Lillie

1 Introduction

Numerical simulations used to predict events are always challenging. Among the challenges is establishing some basis for confidence in the results when no experimental results exist, i.e. a prediction. While there is no assurance that all the necessary physics have been included in the model, e.g. thermal effects, until the experimental results are available for comparison, there are procedures the user can adopt in model development that will build confidence in the modeling.

The first of these confidence building procedures is mesh refinement. In refining the mesh, or key parts of the mesh, the user should see the results of interest converge. The results may not converge to the eventual experimental result, due to possible missing physics, but a convergent model is an indication of a well posed model. Conversely, if the mesh refinement does not produce a converged result this is an indication of an ill posed model.

While some (all too few) users understand the value of mesh refinement, even fewer users appreciate the confidence provided by solving the problem at hand using different solution strategies. Too many users apply the method they know even if alternative, and possibly better, solution techniques exist. LS-DYNA offers a menu of solution strategies and the knowledgeable user takes advantage of multiple solution strategies when predictions are required.

In this manuscript four solution strategies for air blast loading of structures are presented. The techniques are: Load Blast Enhance (LBE), Multi-Material Arbitrary Lagrange Eulerian (MM-ALE), Particle Blast (PB) and Smooth Particle Hydrodynamics (SPH). The first is an engineering model requiring minimal input and with minimal CPU requirements. The latter three are so called 'first principal' models requiring fairly extensive user input, e.g. equations of state of the explosive and air. The computing resources required by these three techniques are substantial.

To provide a platform for comparing these air blast techniques and describing their advantages and disadvantages, two similar experiments, i.e. air blast loading of a metal plate, are modeled. The simulation methods are compared with the experiments and with each other.

The goal is not to tune each method to the provided experimental results, but to use as much as possible an "out-of-the-box" simulation. Then the results can possibly be 'tuned' with the explanation of the tuning invoked. The same target mesh and material model/parameters and explosive (PETN & TNT) EOS where applicable will be used in all four methods.

***KEYWORDS** LOAD_BLAST_ENHANCED, PARTICEL_BLAST, Multi-Material ALE, Smooth particle Hydrodynamics, near-field, near-contact, explosive charges

Note that ***KEYWORDS** may be written with the associated template "keyword".

2 Description of the Experiments

The experiments described in this section are based on the work of Hargather and Settles (2009) and Neuberger et al. (2009). Both sets of experiments involve clamped circular metal plates loaded by bare explosive charges. In one case the charge is quite small, on the order of 0.9grams, and in the other case larger charges of 3.75 and 8.75kg are used. The standoff distance to the metal target

plates are such that the scaled ranges are between $Z=0.06 \text{ kg/m}^{1/3}$ and $Z=0.83 \text{ kg/m}^{1/3}$ the former is considered a near contact charge and thus not applicable for the LBE engineering model. At the more distant scaled range, here termed near field, the target is within the detonation products (fireball) and offers a challenge to blast modeling techniques.

2.1 Hargather and Settles Experiments – Near Field

A thin (0.406mm) aluminum clamped circular plate of diameter 0.25m is exposed to the free air burst of a 0.9g charge of PETN at a standoff of 0.115m; see **Error! Reference source not found.** The charge was in the form of a cylinder with a height to diameter ration of unity. The reported data is the maximum displacement at the center of the plate.

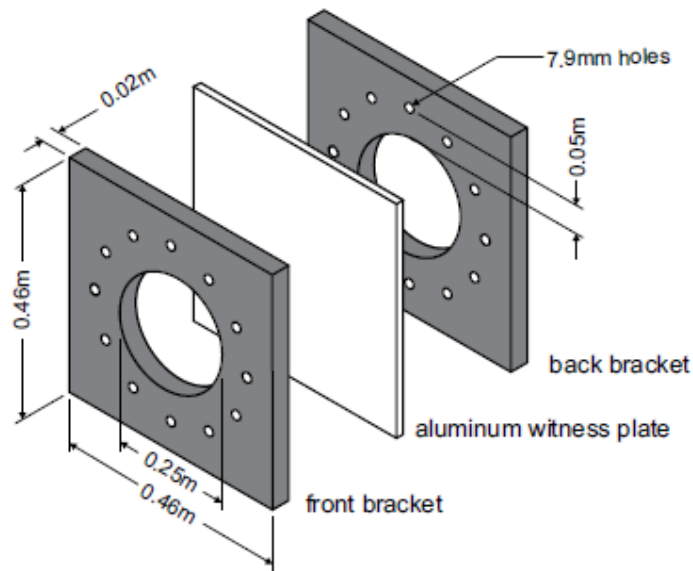


Fig. 1: This is Fig 1 in Hargather and Settles (2009).

Hargather and Settles reported 16 tests with various PETN charge masses and standoff distances – unfortunately only one duplicate test, but three groups of tests with similar scaled ranges; see **Error! Reference source not found.** Overall the scaled ranges varied from $Z=0.36 \text{ kg/m}^{1/3}$ to $Z=1.19 \text{ kg/m}^{1/3}$. An additional 15 test results were reported for the explosive TATP.

Table 1: Selected tests from Table 1 in Hargather and Settles (2009).

$Z \left(m / kg^{1/3} \right)$	Test	PETN (g)	SOD (mm)	Displacement (mm)
0.83	4	0.75	75	10.51
0.83	6	0.89	80	11.10
0.85	7	1.00	85	10.95
0.69	8	0.65	60	10.20
0.68	9	0.70	60	10.54
0.70	11	0.98	70	12.49
0.37	14	0.82	35	15.41
0.37	15	0.88	35	16.57
0.36	16	0.90	35	16.20

The specific tests to be simulated are indicated in bold, but comparisons will be made to the statistic of the corresponding group of three tests:

- Tests 4, 6 & 7: Average Displacement 10.85mm with a coefficient of variation of 2.8%
- Tests 8, 9 & 11: Average Displacement 11.08mm with a coefficient of variation of 11.2%
- Tests 14, 15 & 16: Average Displacement 16.06mm with a coefficient of variation of 3.7%

Clearly the middle group of Tests 8, 9 & 11 has a significantly larger coefficient of variation than the other two groups.

2.2 Neuberger et al. Experiments – Near Contact

A 20mm rolled homogenous armor (RHA) clamped circular steel plate of diameter 1.0m is exposed to the free air bursts of 3.75 and 8.75kg charges of TNT at standoffs of 0.2 and 0.13m, see **Error! Reference source not found.** The corresponding scaled ranges are $Z=0.13 \text{ kg/m}^{1/3}$ to $Z=0.06 \text{ kg/m}^{1/3}$, both ranges are considered to be near contact detonations.

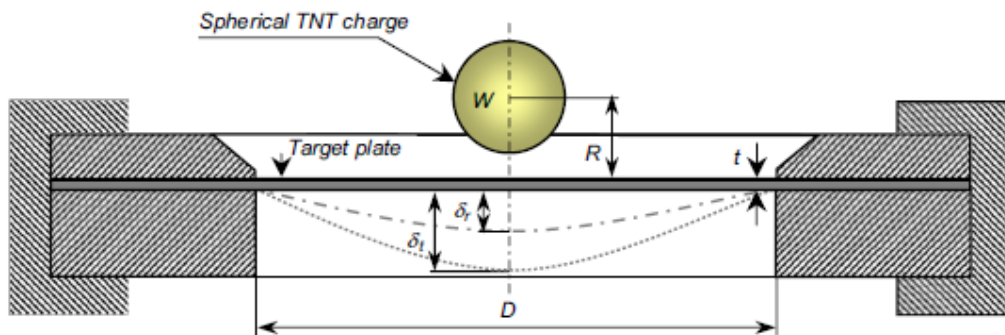


Fig.2: This is Fig 3 in Neuberger et al. (2009).

Error! Reference source not found. is a summary of the three tests reported by Neuberger et al. (2009) for the 20mm thick RHA plate; see their Table 1.

Table 2: Tests from Table 1 in Neuberger et al. (2009)

$Z \left(m / kg^{1/3} \right)$	Test	TNT (kg)	SOD (mm)	Displacement (mm)	
				Experiment	Numerical
0.13	a	3.75	200	54.0	52.4
0.10	b	8.75	200	107.0	104.8
0.06	c	8.75	130	165.0	123.0

In an earlier work, Neuberger et al. (2007), the authors reported results for the same RHA plate of 1m diameter with thicknesses of 0.01 and 0.02m loaded by spherical charges varying between 0.47 and 8.75kg at standoff distances varying between 0.07 and 0.2m. Again all the scaled ranges were between $Z=0.06 \text{ kg/m}^{1/3}$ to $Z=0.13 \text{ kg/m}^{1/3}$, i.e. near contact detonations. Although there were no duplicate tests, the same scaled ranges were repeated for the 10mm thick RHA plate.

3 Simulation of the Hargather and Settles Experiments – Near Field

The aluminum target plates were described by Hargather and Settles (2009) as

“Aluminum alloy 3003, 0.406 mm thickness, was used here as the witness-plate material. The aluminum was purchased from McMaster-Carr, Inc., and had quoted yield strength of 144.8 MPa and a Brinell hardness of 40, meeting manufacturing standard ASTM B209.”

The material properties were obtained in part from *www.matweb.com* for Aluminum3003-H14 and used with LS-DYNA's *MAT_PLASTIC_KINEMATIC – Note: units are grams-millimeters-milliseconds with a derived stress unit of MPa.

```
*MAT_PLASTIC_KINEMATIC_TITLE
Aluminum 3003-H14 (www.matweb.com)
$# mid ro e pr sigy etan beta
    1222 2.73E-3 68.9E3 0.33 145.0 50.0
$# src srp fs vp
    0.000 0.000 0.000 0.000
```

With the tangent modulus estimated from the provided yield and ultimate stress using an elongation at failure of 10%: ETAN= (150-145)/0.1 = 50 MPa, i.e. essentially no strain hardening.

The PETN parameters for the Jones-Wilkins-Lee (JWL) EOS were obtained from the LLNL Explosives Handbook (Dobratz, 1981) for a density of 1.77×10^{-3} g/mm³

```
*MAT_HIGH_EXPLOSIVE_BURN
$ MID RO D PCJ BETA
    2080, 1.77E-3, 8.30e3, 3.35E4, 0.0

*EOS_JWL
$ EOSID A B R1 R2 OMEG E0 V0
    2080 , 6.17E5, 16.926E3, 4.4, 1.20, 0.25, 10.1E3, 1.0
```

The air surrounding the target plate and explosive was modeled using LS-DYNA's EOS_LINEAR_POLYNOMIAL as an ideal gas with an initial pressure of one atmosphere (0.1 MPa):

```
$ Properties for Air
$
*MAT_NULL
$ MID RO PC MU TEROD CEROD YM PR
    100, 1.29e-6, 0.0, 0.0, 0.0, 0.0
$ EOS CARDS
$ Properties for Air
$
*EOS_Linear_Polynomial
$ EOSID C0 C1 C2 C3 C4 C5 C6
    100 , 0.0, 0.0, 0.0, 0.0, 0.4, 0.4, 0.0
$ e0 v0
    0.25, 1.0
```

The circular plates were modeled using shell elements, ELFORM=2 Belytschko-Tsay, with five through thickness integration points¹. shows the quarter symmetry butterfly shell mesh with nominal 5mm elements. The nominal size is determined by dividing the square core of the butterfly mesh by the number of shell elements along that edge, e.g. 5mm = 31.25/6. In addition to the nominal 5mm mesh, similar meshes were created at 10 (3 elements) and 2.5mm (12 elements) for mesh convergence studies.

¹ Increasing the number of through thickness integration points to 9, did not change the center displacement.

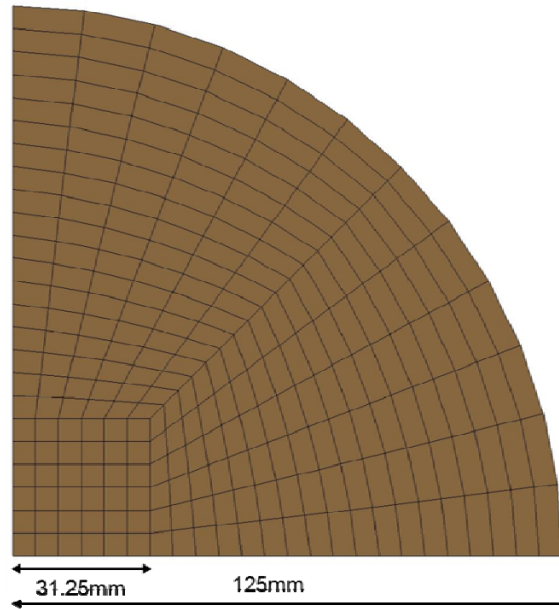


Fig.3: Quarter circle butterfly mesh – nominal 5mm elements.

3.1 Load Blast Enhanced Results

The engineering model Load Blast Enhanced is based on the Kingery-Bulmash (1984) relations for free air blast from spherical and hemi-spherical surface charges of TNT; these are the same air blast relations provided in UFC 3 340 02 and the often cited ERDC application ConWep. In addition to being limited to equivalent TNT charges, the Kingery-Bulmash relations are restricted to scaled ranges greater than about $0.4 \text{ m/kg}^{1/3}$, or about three times the charge radius.

The limitation of use with only TNT charges is often mitigated by specifying an equivalent amount of TNT, e.g. the amount of TNT that would produce the same blast wave parameter as say PETN. The blast wave parameter is often maximum pressure or maximum impulse, and differing TNT equivalents will apply to each blast wave parameter. For example, for the explosive C-4, ConWep provides TNT equivalences of 1.37 for maximum pressure and 1.19 for maximum impulse; ConWep does not provide equivalences for PETN.

Two items often ignored in these TNT equivalences are (1) the range at which the equivalences are to be formed, i.e. TNT equivalences are a strong function of range from the charge, and (2) the difference in incident and reflected pressure and impulse equivalences. Both of these are important in blast loaded structures as there is no 'standard' range to a target and targets typically respond to reflected pressure and especially impulse, rather than incident blast wave parameters.

Hargather and Settles (2007) cite TNT equivalences for PETN of between 0.7 and 1.8 depending on the range to the target; see **Error! Reference source not found.** They also cite Kinney & Graham (1985) as providing TNT equivalences for PETN of 1.2 to 1.8. But both sets of TNT equivalences are based on maximum incident pressure. What is needed for the present plate deformation simulations is the TNT equivalence for impulse, especially reflected impulse.

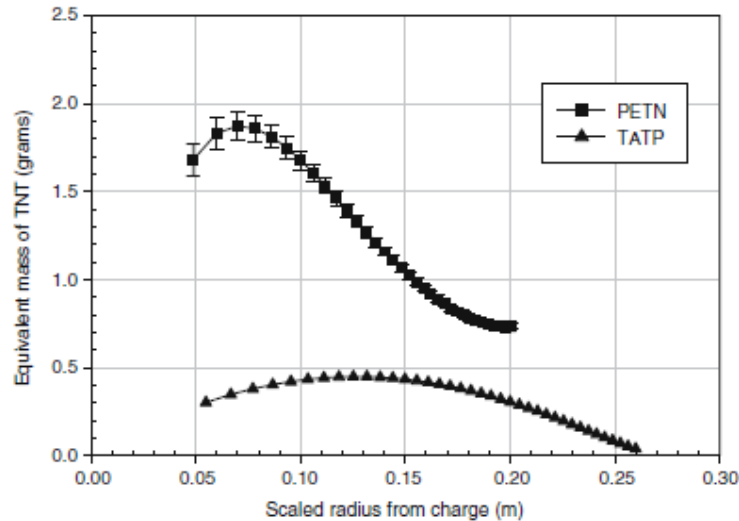


Fig.4: TNT equivalences for 1g of PETN and TATP; this is Fig. 10 in Hargather & Settles (2007)

In addition to reporting the experimental maximum center displacement, Hargather and Settles (2009) provided estimates of the incident impulse for the various PETN masses and standoff distances in their Table 1². For example, at the largest standoff distance reported: Test 1 at 0.115m with 0.9g PETN, $Z=0.36 \text{ kg/m}^{1/3}$, the average incident impulse was 21.4 Pa-s.

As a check on these reported TNT equivalencies, ConWep was run at the fixed distance of 0.115m with varying TNT charge masses until the incident impulse was matched. This occurred for a TNT mass of 1.7g yielding a TNT equivalence of 1.89; Note: this is on the upper end of the above cited TNT equivalences for maximum incident pressure; see **Error! Reference source not found.** However, using this TNT equivalence with LOAD_BLAST_ENHANCED produced a plate central displacement of 16.6mm well in excess of the experimentally observed displacement of 7.55mm.

All this points to the 'Achilles heel' of LOAD_BLAST_ENHANCED:

"What TNT equivalence is to be used?"

To demonstrate the variability of TNT equivalence with scaled range, for the three scaled ranges listed in **Error! Reference source not found.** and the above mentioned Test 1, the TNT equivalence was adjusted until the computed center displacement agreed with the experimental observation. **Error! Reference source not found.** summarizes the results of this parameter study. For the three tests at scaled ranges less than unit, i.e. Test 15, Test 8 and Test 6, and thus likely inside the detonation products, there is not much variation in the TNT equivalence across a fairly wide range of scaled distances. However for Test 1, at the largest scaled range reported by Hargather & Settles (2009), and most likely outside the detonation products, the TNT equivalence is quite low, and much lower than the values cited above for maximum incident pressure, i.e. between 0.7 and 1.8.

² These impulse values were measured in a previous effort by the authors: Hargather and Settles (2007).

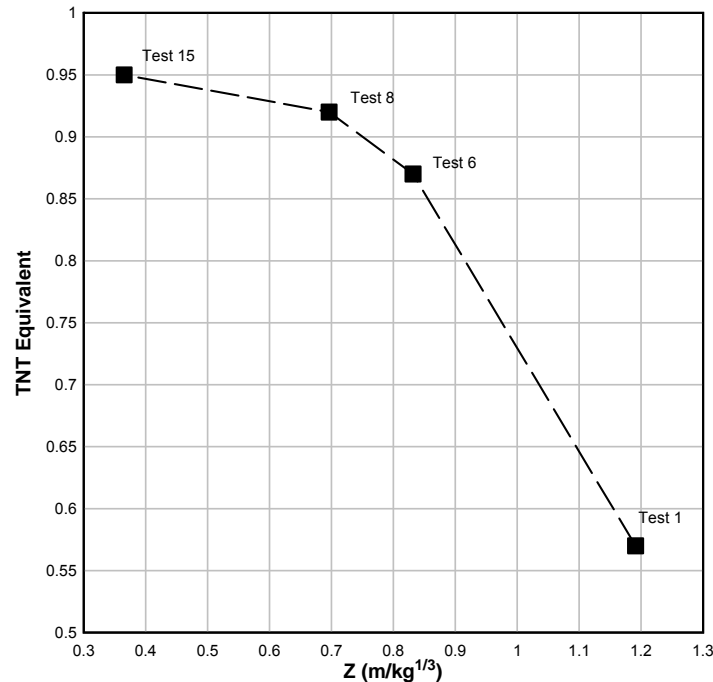


Fig.5: TNT equivalences for PETN at four scaled ranges adjusted to agree with Hargather & Settles (2009) central plate displacement test results.

LOAD_BLAST_ENHANCED should always be the analyst's first choice when attempting blast loading predictions. This engineering model is computational efficient and while the associated results will depend on the choice of the TNT equivalence, the ability to simulate the target response of interest efficiently provides both a target model debugging feature and insights to the anticipated structural response when the more complex 'first principal' methods are used subsequently.

3.2 Multi-Material ALE Results

Three dimensional Multi-Material ALE (MM-ALE) simulations were performed for the three tests listed in **Error! Reference source not found.** Only two mesh refinements were attempted using 5 and 2.5mm uniform mesh spacing for the air domain with corresponding to the 5 and 2.5mm plate meshes described previously. **Error! Reference source not found.** shows the typical configuration of the MM-ALE models. The air domain has a radius of 375mm and a total height of 500 mm. This height is divided into two air domains: 300mm below the target plate and 200mm above the target plate, see **Error! Reference source not found.** Using two such air domains allows for easy visualization of any leakage of the lower air into the upper air through the plate.

The fluid-structure interaction was modeled with three *CONSTRAINED_LAGRANGE_IN_SOLID keywords, one for the detonation products and one each for the upper and lower air. The following keyword parameters were used: DIREC=2, PFAC=0.1, ILEAK=2, PFACMM=4 and THKF=0.406mm (plate thickness).

Since the air domains are relatively coarsely meshed, compared to the size of the small approximately 1g PETN charges, it was decided to initialize the 3D domains using the LS-DYNA 1D-to-3D mapping. This allowed for a fine mesh of 0.05mm cells for simulating the detonation of the PETN charge. The rule-of-thumb is a minimum of 10 elements across the radius of the charge with 20 being a reasonable number. For these nearly 1g charges, the 0.05mm 1D spherical calculations included more than 80 elements across the charge radius. The 1D spherical calculations were terminated a few (3D) elements before the shock wave arrived at the target plate to provide for consistent mapping of the 1D pressure field onto the 3D mesh.

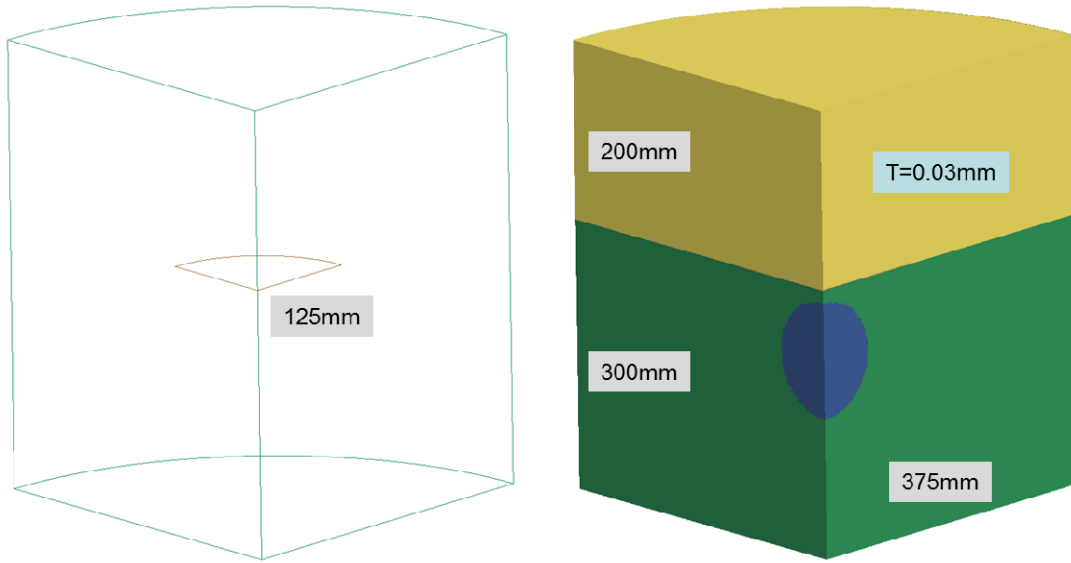


Fig.6: Typical 3D MM-ALE initial mesh configuration.

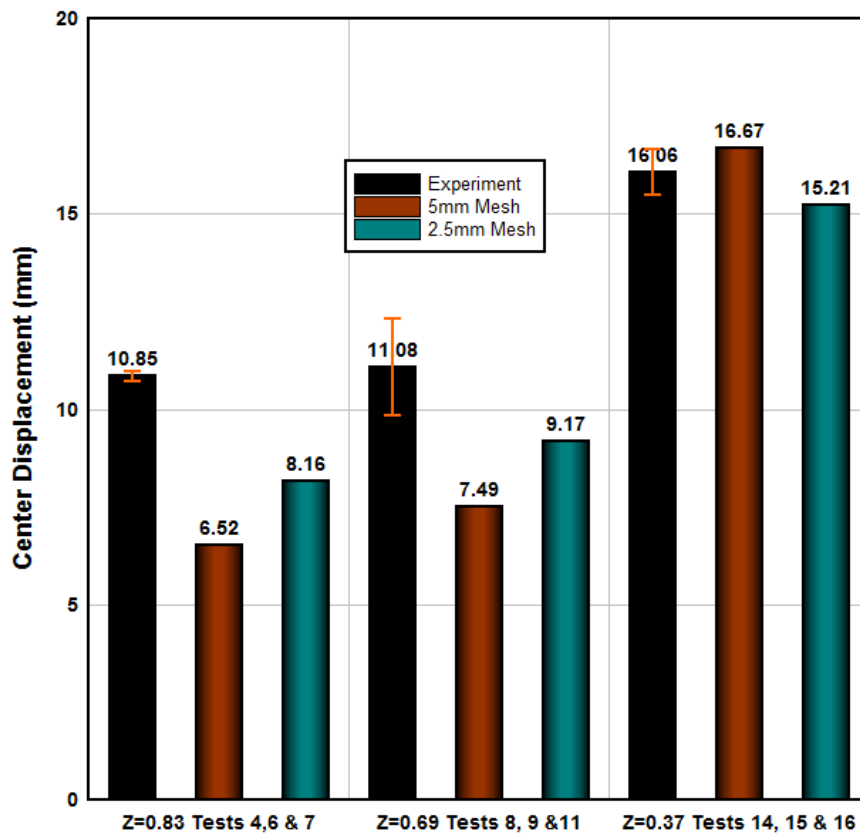


Fig.7: Comparison of plate center maximum displacement for three near-field scaled ranges.

Error! Reference source not found. is a bar chart comparing the average plate central displacements from the test groups listed in **Error! Reference source not found.** with the MM-ALE results using the 5 and 2.5mm meshes. The test data include 'error bars' of one standard deviation on either side of the average displacement. The 2.5mm MM-ALE results should not be considered as

converged, as another mesh refinement is desirable. However, the 686,400 solid elements in the 2.5mm spacing mesh were already taxing the locally available computing resources.

Generally, as the scaled distance decreases, i.e. going from $Z=0.83$ to $Z=0.37 \text{ m/kg}^{1/3}$, the MM-ALE results are in better agreement with the experimental results.

3.3 Particle Blast Results

Particle blast simulations were performed for the three tests. The particle blast method, which is a Lagrangian approach, modeled the high explosive detonation products and air as a set of discrete spherical particles that transfer force between each other through collisions. The pressure applied to structures is numerically represented by the momentum transfer as particles impact and rebound from the surface of the structure. Similar to the above described MM-ALE simulations, two mesh refinements were attempted using 5 and 2.5mm uniform plate meshes. The air domain has a length, a width, and a total height of 500mm. The height is divided into two domains: 300mm below the target plate and 200mm above the target plate, see **Error! Reference source not found.**

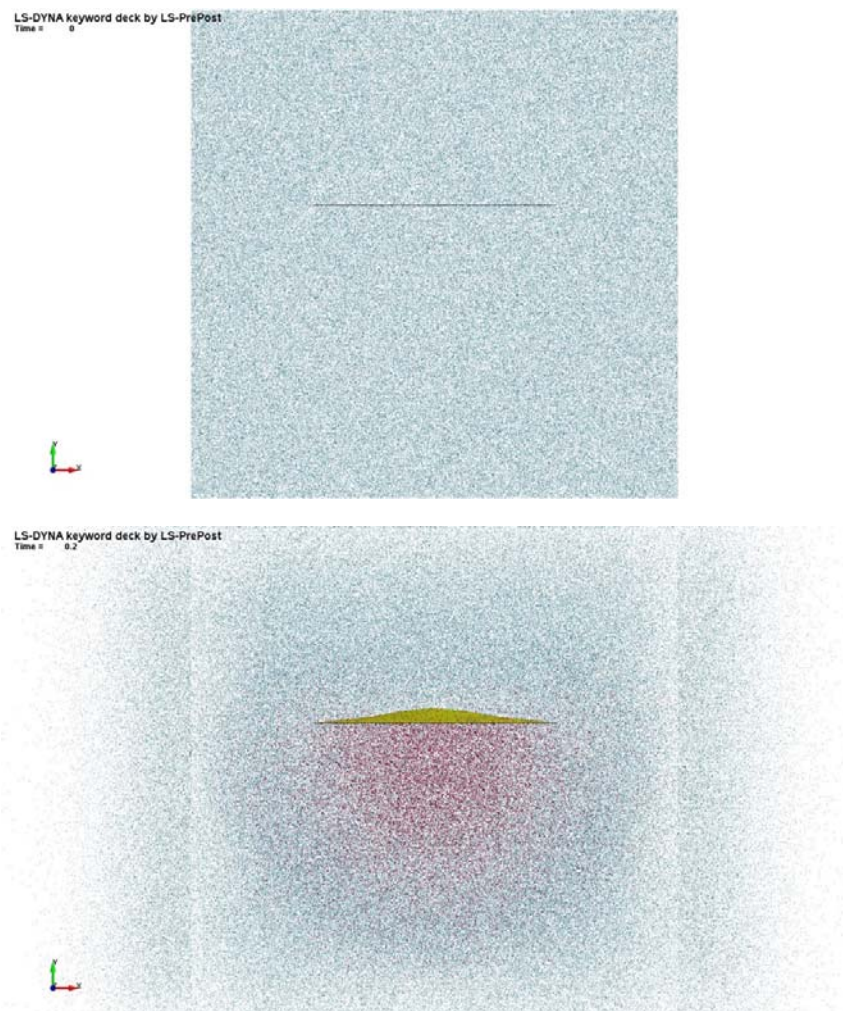


Fig.8: The initial configuration and 0.1ms after detonation.

The PETN explosive was modeled by (explosive) particles. The parameters for defining a particle blast model of a high explosive are the detonation velocity D , initial density ρ , initial energy density E , the ratio between heat capacities at constant pressure and volume γ , and co-volume effect parameter b . Of the five constants, three (the detonation velocity D , density ρ , and energy density E) can be directly

obtained from the PETN parameters for the JWL EOS. The heat capacities ratio γ was derived from JWL EOS as $\gamma = 1 + \text{OMEG}$. The co-volume effect parameter b is considered here to better represent the gas behavior at extremely high pressures and used as an *adjustable* parameter. The parameters for defining PETN are given in **Error! Reference source not found.**

Table 3: Particle explosive parameters for PETN

D(m/s)	$\rho(\text{kg/m}^3)$	E(J/m ³)	γ	b
8300	1770	10.1E9	1.25	0.3

The air surrounding the target and explosive were modeled as an idea gas, the corresponding parameters for air particles are given in **Error! Reference source not found.**

Table 4: Particle parameters for Air

$\rho(\text{kg/m}^3)$	E(J/m ³)	γ
1.27	2.53E5	1.4

The number of air particles and the number of explosive particles are selected such that the mass of an air particle is approximately equal to the mass of an explosive particles. For the 5mm model, 5,000 explosive particles and 891,834 air particles were used to model the PETN charge and air, respectively, while for the 2.5mm model, 40,000 explosive particles and 7,134,672 air particles were used, respectively.

The predicted plate center maximum deflections are given in **Error! Reference source not found.**, and compared with the experimental results from Test 6, 8, and 15.

Table 5: Comparison with experimental results

Z	Test	PETN(g)	SOD(mm)	Displacement(mm)		
				Experiment	Numerical(5mm)	Numerical(2.5mm)
0.83	6	0.89	80	11.10	11.63	12.30
0.69	8	0.65	60	10.20	10.75	11.40
0.37	15	0.88	35	16.57	15.67	16.84

3.4 Smooth Particle Hydrodynamics Results

Smooth Particle Hydrodynamics (SPH) results were planned for both series of experiments, i.e. Hargather & Settles and Neuberger et al., but these simulations proved more challenging than for the other three solution methods. At the time this manuscript was prepared, only results corresponding to Test 6 from the Hargather & Settles series were available.

The SPH method has previously successfully been used for solving fluid (liquid) structure and soil structure interaction problems. The method has been used for problems involving pressure wave propagation through a relatively dense media and its interaction with structures. The present application is to a much less dense media, i.e. air, and presented challenges for the SPH method.

Starting from a 3D hexahedra fine mesh for the air and high explosive material, where the nominal mesh size is around 2.5 mm, an SPH mesh was constructed using the solid-to-SPH meshing capabilities of LS-PREPOST. For the target plate, a 5mm mesh, similar to that described above in the Hargather & Settles simulation section, was used for the plate. The air and high explosive materials were modeled using approximately 125.000 particles, with a particle spacing of 2.5 mm. The mass of the explosive is 0.89grams located at a distance 80mm for the center of the plate; this is Test 6 as listed in **Error! Reference source not found.**

Using the two planes of axial symmetry from the experiment, only one quarter of the problem was modeled. **Error! Reference source not found.** illustrates the SPH and Lagrange-shell models for the

air-explosive and the target plate. A new version of LS-DYNA LS971 was used to simulate the problem up to termination time of 1ms.

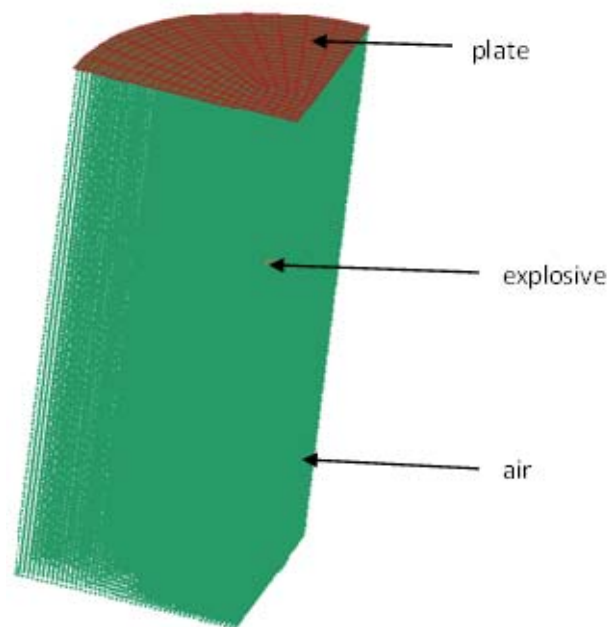


Fig.9: SPH model for Air and Explosive and Lagrange shell mesh for the plate

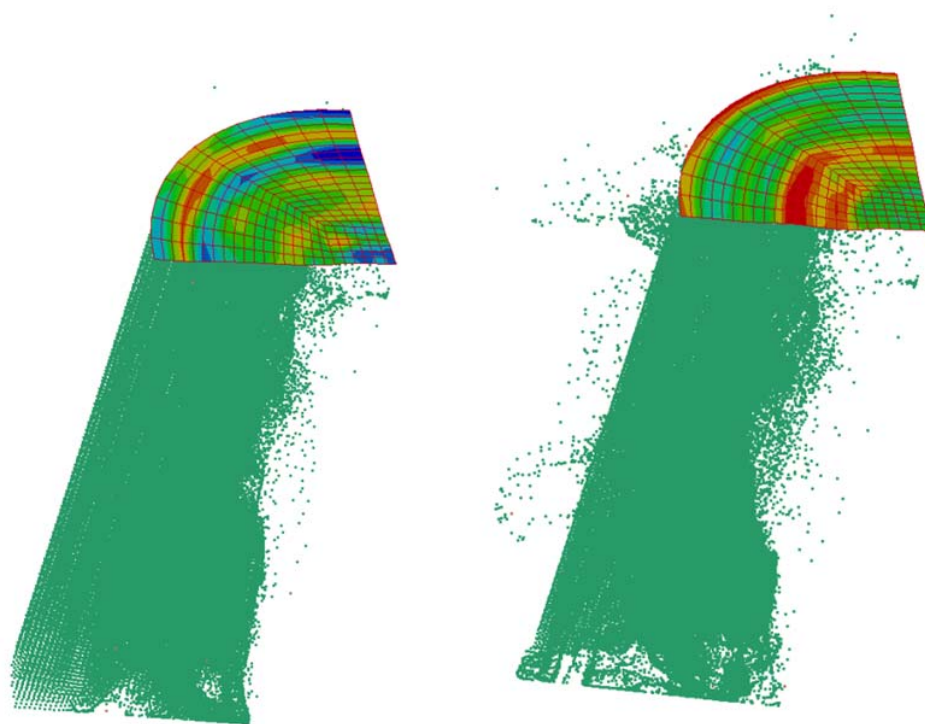


Fig.10: Von Mises stresses and deformed configurations at 0.5 (left) and 1ms (right).

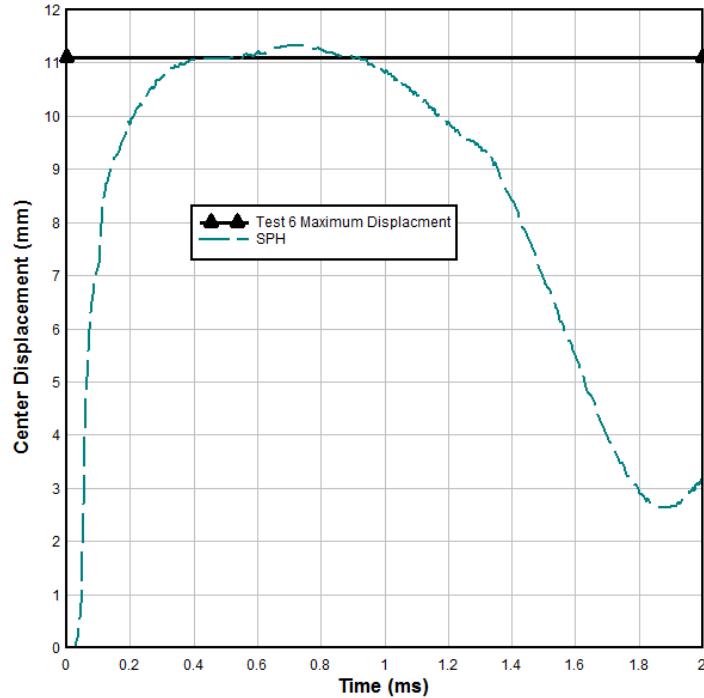


Fig. 11: Displacement history at center of the plate.

4 Simulation of the Neuberger et al. Experiments – Near Contact

The rolled homogeneous Armor (RHA) target plates were described by Neuberger et al. (2009)

The plate material (RHA steel) was modeled as a rate-sensitive elastic–plastic bilinear material obeying Von Mises yield criterion. Generally, this material model is suitable to model isotropic and kinematic hardening plasticity. Strain-rate effects are accounted for based on the Cowper–Symonds model.

The LS-DYNA *MAT_PLASTIC_KINEMATIC material model was used with the properties provided in Neuberger et al. – Note: units are grams-millimeters-milliseconds with a derived stress unit of MPa.

```
*MAT_PLASTIC_KINEMATIC_TITLE
RHA - Neuberger (2009)
$#      mid      ro      e      pr      sigy      etan      beta
      1223  7.838E-3  212.0E3  0.28  1200.0  6500.0
$#      src      srp      fs      vp
      0.300    5.000    0.000    1.000
```

The TNT explosive properties were obtained from the LS-DYNA User Manual Volume II in the section describing EOS_JWLb.

```
*MAT_HIGH_EXPLOSIVE_BURN
$ MID      RO      D      PCJ      BETA
      8, 1.631E-3, 0.67174E4, 0.18503E5, 0.0
$
$
$      EOS CARDS
$
$      TNT
*EOS_JWLb
$ EOSID      A1      A2      A3      A4      A5
```

```

      8, 490.07e5, 56.868e5, 0.82426e5, 0.00093e5
$  R1      R2      R3      R4      R5
  40.713, 9.6754, 2.4335, 0.15564
$  AL1      AL2      AL3      AL4      AL5
  0.00, 11.468
$  BL1      BL2      BL3      BL4      BL5
  1098.0, -6.5011
$  RL1      RL2      RL3      RL4      RL5
  15.614, 2.1593
$  C      OMEGA      E      V0
  0.0071e5, 0.30270, 0.06656e5, 1.0

```

The air surrounding the target plate and explosive was modeled using LS-DYNA's EOS_LINEAR_POLYNOMIAL as an ideal gas with an initial pressure of one atmosphere (0.1 MPa); the air material model parameters were provided in the description of the Hargather & Settles models.

The circular plates were modeled using three element types:

1. Axisymmetric beam elements – uniform meshes of 10, 5, 2.5 and 1mm.
2. Axisymmetric shell elements – uniform 4x4mm mesh.
3. 3D shell elements – uniform meshes of 20 and 10mm; similar to the meshes used in the Hargather & Settles simulations.

The axisymmetric beam elements used ELFORM=8 with 2x2 Gauss quadrature (QR=2) and a thickness corresponding to the 20mm RHA target plate.

The axisymmetric shell elements used ELFORM=14 with four elements through the 20mm target plate thickness and 125 elements along the 500mm radius of the circular target plate.

The 3D shell element meshes used ELFORM=2 Belytschko-Tsay, with five through thickness integration points. **Error! Reference source not found.** shows the quarter symmetry butterfly shell mesh with nominal 20mm elements. The nominal size is determined by dividing the square core of the butterfly mesh by the number of shell elements along that edge, e.g. 20mm = 125/6. In addition to the nominal 20mm mesh, a similar mesh was created at 10mm (12 elements) for mesh convergence studies.

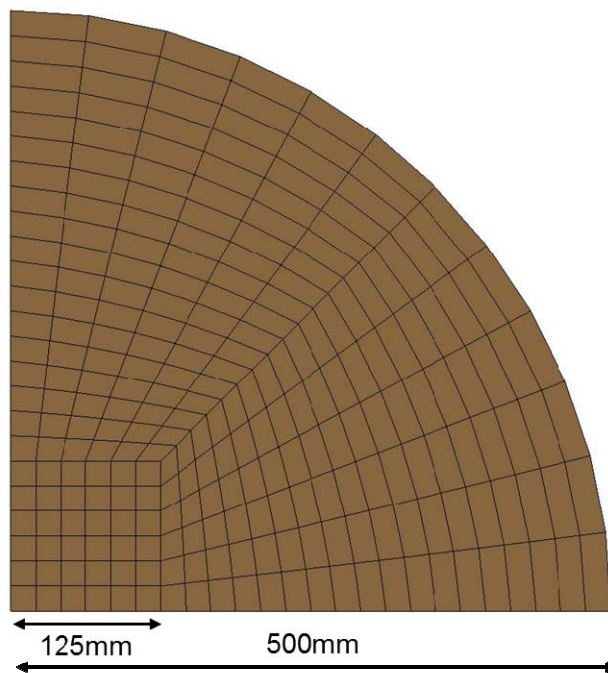


Fig. 12: Quarter circle butterfly mesh – nominal 20mm elements.

4.1 Load Blast Enhanced Results

For these close-in scaled ranges, i.e. $0.06 < Z < 0.13 \text{ m/kg}^{1/3}$ the LS-DYNA LOAD_BLAST_ENHANCED algorithm issues the warning message:

```
*** Warning 40935 (SOL+935)
Segment too close to charge.
*LOAD_BLAST equations may not be valid.
```

Indicating the scaled range is less than the minimum required for using the Kingery & Bulmash air blast relations. Recall the rule-of-thumb is the target should be at least three charge radii from the center of the charge. For the 3.75 and 8.75kg TNT charges, three times the radius is 245 and 325mm, respectively. Thus standoffs distance of 200 and 130mm are too close for LOAD_BLAST_ENHANCED to be applied reliably. Note: the LOAD_BLAST_ENHANCED algorithm continues the simulation after issuing the warning, applying some type of blast loading, but users are advised to observe the warning and not rely on these results.

However, Neuberger et al. Stated:

“Simulations were carried out using LS-DYNA finite element code [24]. A pure Lagrangian approach was adopted, together with a simplified engineering blast model of a spherical charge to reduce the calculation time.

The ‘load-blast’ function implemented in LS-DYNA is based on an implementation by Randers-Pehrson and Bannister [29] of the empirical blast loading functions by Kingery and Bulmash [25] that were implemented in the US Army Technical Manual ConWep Code [26].”

Implying that the LS-DYNA LOAD_BLAST algorithm was used. The lead author was contacted via email and responded:

“It is true that the basic LOAD_BLAST function will not provide the results presented in our paper, however we have developed an additional application (a type of a factor to the LOAD_BLAST function) to meet the close range blast effects, based on previous test results.”

Thus readers of the Neuberger et al. references are cautioned that the reported engineering model results, which agree quite well with the experimental measurements, were not generated using the LS-DYNA LOAD_BLAST algorithm.

4.2 Multi-Material ALE Results

Error! Reference source not found. shows the initial configuration of the axisymmetric models, with beam elements used to model the 0.50m radius target plate. As was done for the Hargather & Settles MM-ALE models, the air domain is divided into two regions: above the target plate (0.20m) and below the target plate (1.20m).

This figure also provides a visual indication of just how close to the target plates these near contact TNT charges were placed in the tests.

The fluid-structure interaction was again modeled with three *CONSTRAINED_LAGRANGE_IN_SOLID keywords, one for the detonation products and one each for the upper and lower air. The same keyword parameters as used for the Hargather & Settles models were used with the THKF parameter updated for the 20mm RHA target plate.

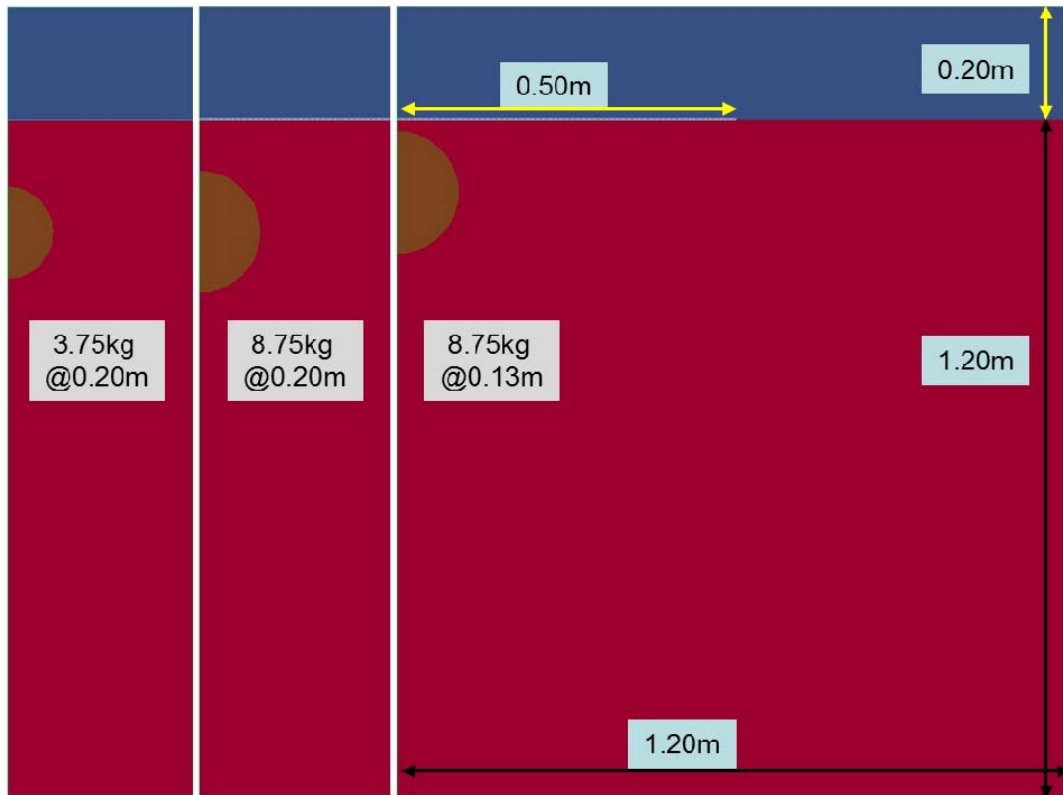


Fig.13: Initial configuration of the axisymmetric MM-ALE models.

Figure 1 is a bar chart comparing the average plate central displacements from the tests listed in **Error! Reference source not found.** with the MM-ALE results using the 10, 5 and 2.5mm axisymmetric beam element meshes, a 4mm axisymmetric shell element mesh, and 10mm 3D shell element mesh. There are no test data 'error bars' as only one test per configuration was reported. The lack of repeated tests makes the data less than ideal for validation purposes, but it does provide a baseline for comparing the numerical methods. The 2.5mm MM-ALE axisymmetric beam element results may be considered as converged, however another mesh refinement is desirable. Similarly, additional axisymmetric shell elements results are desirable.

The general trend in these MM-ALE results is as the scaled range decreases from $Z=0.13\text{m/kg}^{1/3}$ to $Z=0.06\text{m/kg}^{1/3}$ the absolute difference between the experiment and simulated plate displacements increases. However, the relative error remains about the same in the neighborhood of 40%. One postulated cause for this discrepancy is the lack of an after burning model in the LS-DYNA JWL EOS. Such an after burning model would add energy (heat of combustion) to the detonation products, which are the primary fluid loading the plates for these near contact charges.

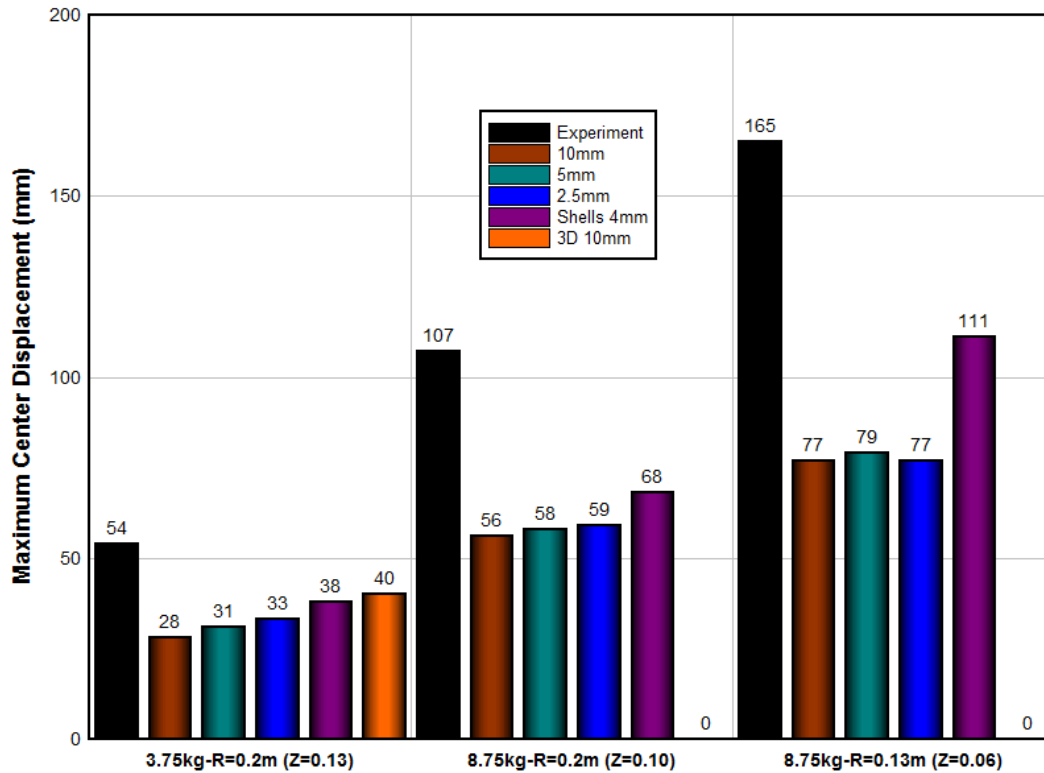


Figure 1 Comparison of plate center maximum displacement for three close-in scaled ranges.

4.3 Particle Blast Results

Particle blast simulations were performed for the three tests using 3D shell elements for the target plates. Meshes similar to those used in the Hargather & Settles simulations with two mesh refinements were attempted using 10mm and 20 mm uniform plate meshes. The air domain has a length and a width of 3m, and a total height of 2m. The height is divided into two domains: 1m below the target plate and 1m above the target plate, see **Error! Reference source not found.**

The TNT charge was modeled by 40,000 explosive particles for the 10mm model, and 5,000 explosive particles for the 20mm model. The corresponding parameters for TNT are given in **Error! Reference source not found.**

Table 6: Particle explosive parameters for TNT

D(m/s)	$\rho(\text{kg/m}^3)$	E(J/m ³)	γ	b
6930	1630	7.0E9	1.3	0.3

Similar to the Hargather & Settles simulations, the number of air particles was selected such that the mass of an air particle is approximately equal to the mass of an explosive particle.

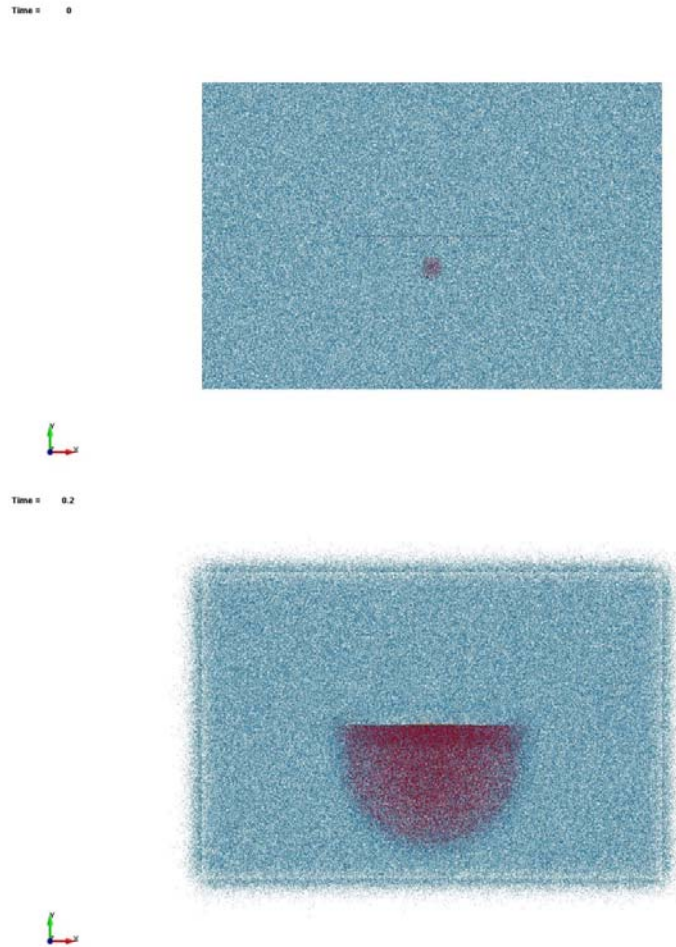


Fig. 14: The initial configuration and 0.2ms after detonation.

The predicted plate center maximum deflections are presented in **Error! Reference source not found.**, and compared with the experimental results.

Table 7: Comparison with experimental results

Z	Test	TNT(kg)	SOD(mm)	Displacement(mm)		
				Experiment	Numerical(20mm)	Numerical(10mm)
0.13	a	3.75	200	52.4	35.9	35.1
0.10	b	8.75	200	107.0	61.0	61.3
0.06	c	8.75	130	165.0	93.1	92.9

The numerical results show that the 20mm particle blast results are converged, i.e. as shown in **Error! Reference source not found.**, the 10mm results are almost identical with the 20mm results.

It is also to be noted that the particle blast results agree with the MM-ALE results, however, both numerical methods predict a smaller maximum deflection than observed in the experiments.

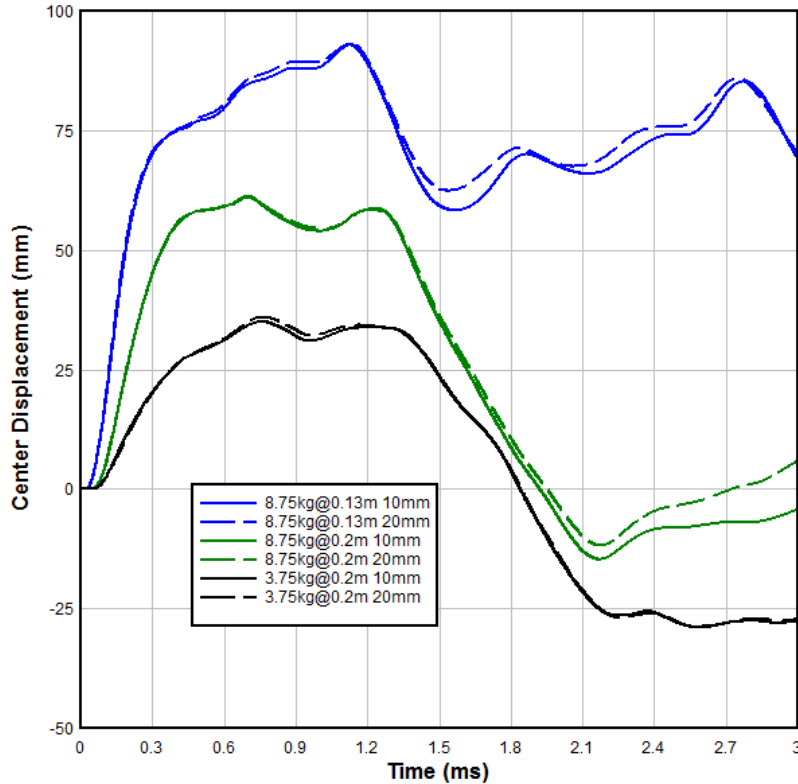


Fig.15: Center displacement-time curve from simulations of test cases with 10mm and 20mm plate mesh.

5 Summary

This section provides a summary of the experimental results and the corresponding simulations. The reader is reminded that the goal of this effort is not to ‘tune’ a given solution technique to the experimental results, but rather to illustrate how a suite of solution techniques can be used to establish some confidence in a simulation when no experimental result is available, i.e. a predictive simulation.

5.1 Hargather and Settles – Near Field Explosions

Error! Reference source not found. is a bar chart summary comparison of the Hargather & Settles near field experimental results – average of three tests with nearly identical scaled ranges – and the corresponding simulation results for the four solution techniques demonstrated. The experimental results are shown with ‘error bars’ of one standard deviation computed for the three similar scaled range tests, as indicated on the abscissa.

The PARTICLE_BLAST results agree quite well with the average experimental measurements, especially when the standard deviations of the data are considered. The largest relative error, a 9% under prediction, occurs at the intermediate scaled range of $Z = 0.69m/kg^{1/3}$, although the PARTICLE_BLAST predicted value is within one standard deviation of the experimental results.

The LOAD_BLAST_ENHANCED results shown in this comparison all used a TNT equivalency of 1.1 times the mass of the PETN charge. As indicated previously in Figure 5, a TNT equivalency of 1.1 is an over estimate of the TNT equivalency needed to match the impulses measured by Hargather & Settles. Thus the LOAD_BLAST_ENHANCED results over estimate the maximum central plate displacement.

The MM-ALE results consistently under predict the experimental results, although the degree of under prediction lessens as the scaled range increases. A careful investigation of the amount of leakage due to the fluid-structure interaction algorithm might be the cause of the near field MM-ALE under predictions.

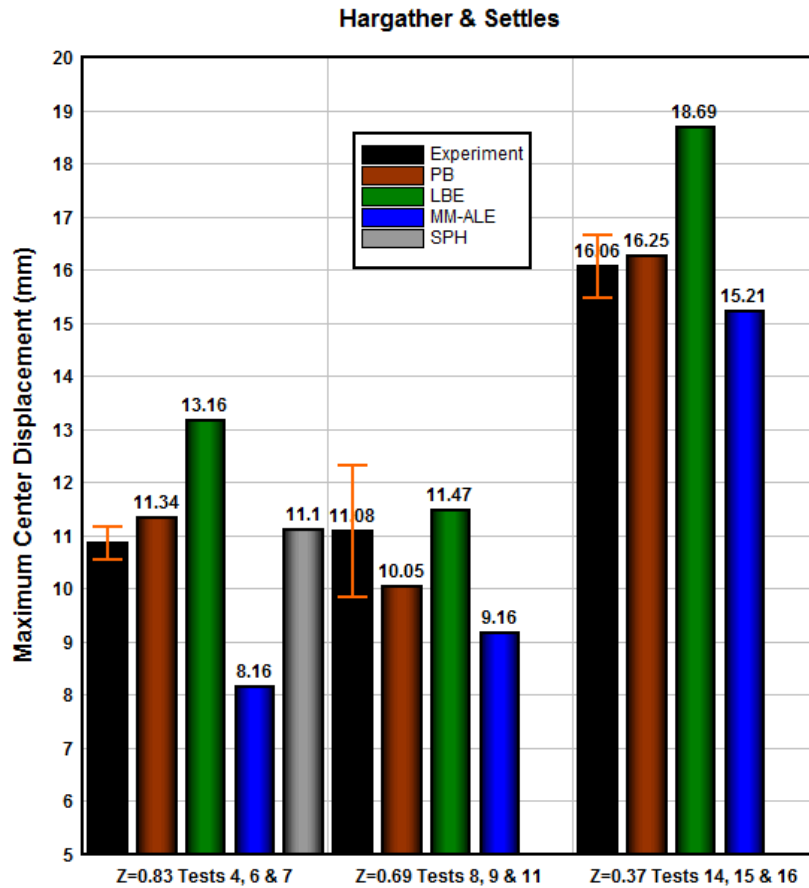


Fig. 16: Summary of Hargather & Settles results and simulations.

5.2 Neuberger et al. – Close in (Near Contact) Explosions

Figure 2 is a bar chart summary comparison of the Neuberger et al. near contact experimental results and the corresponding simulation results for the three solution techniques demonstrated. There are no 'error bars' on the experimental results as there were no repeat tests, nor tests that could be reasonably grouped together. The reader is thus warned not to take the reported experimental results as necessarily being representative of what would have happened with repeat testing.

All the simulation results under predict the experimental maximum plate displacements by about 35% - a significant difference. Somewhat oddly, the solution technique that appears to have the minimum under prediction is LOAD_BLAST_ENHANCED. This is odd in that all three scale ranges are less than the recommended limit for using LOAD_BLAST_ENHANCED.

Excluding the LOAD_BLAST_ENHANCED results, the PARTICLE_BLAST and MM-ALE results, both axisymmetric and 3D, provide fairly consistent predictions of the maximum displacement; although as already mentioned, all under predictions for these near contact charges.

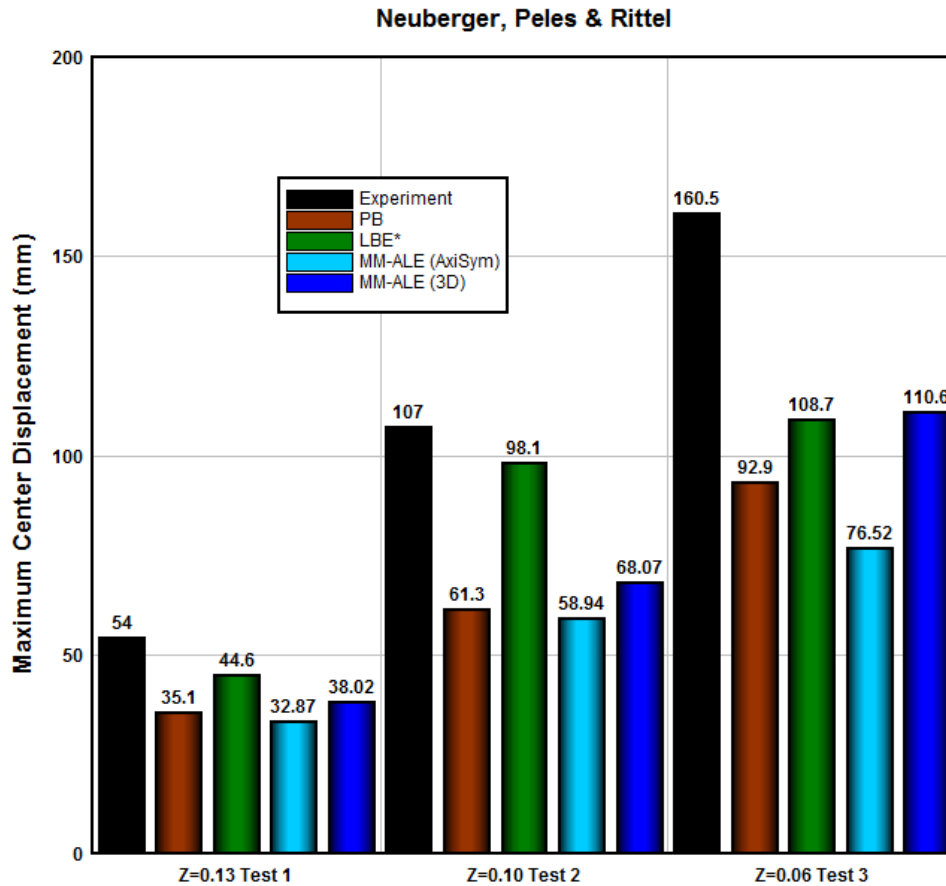


Figure 2 Summary of Neuberger et al. results and simulations.

6 References

Hargather, MJ and GS Settles, (2009) "Laboratory-scale techniques for the measurement of a material response to an explosive blast," *International Journal of Impact Engineering* Volume 36, Pages 940–947.

Hargather, MJ and GS Settles (2007), "Optical measurement and scaling of blasts from gram-range explosive charges," *Shock Waves*, Volume 17, Pages 215–23.

Kingery, C. N. and Bulmash, G., Airblast Parameters From TNT Spherical Air Bursts and Hemispherical Surface Bursts, ARBRL-TR-02555, April 1984.

Kinney, G.F., Graham, K.J.: Explosive Shocks in Air. Springer, New York (1985)

Neuberger A, S.Peles, and D.Rittel, (2009) "Springback of circular clamped armor steel plates subjected to spherical air-blast loading," *International Journal of Impact Engineering*, Volume 36, Issue 1, January, Pages 53–60.

Neuberger A, S. Peles, and D. Rittel, (2007), "Scaling the response of circular plates subjected to large and close range spherical explosions. Part I: air-blast loading," *International Journal of Impact Engineering*, Volume 34, Number 5, Pages 859-873.